

## BRIEF COMMUNICATION



# Truncating variants in the penultimate exon of *TGFBR1* escaping nonsense-mediated mRNA decay cause Loey-Dietz syndrome

Paola Fortugno<sup>1,2,9</sup>, Rosanna Monetta<sup>3,9</sup>, Valeria Cinquina<sup>4</sup>, Chiara Rigon<sup>5,6</sup>, Francesca Boaretto<sup>5,6</sup>, Chiara De Luca<sup>3</sup>, Nicoletta Zoppi<sup>4</sup>, Luana Di Leandro<sup>3</sup>, Emanuela De Domenico<sup>7</sup>, Arianna Di Daniele<sup>3</sup>, Rodolfo Ippoliti<sup>3</sup>, Francesco Angelucci<sup>3</sup>, Ernesto Di Cesare<sup>3</sup>, Ruggero De Paulis<sup>8</sup>, Leonardo Salviati<sup>5,6</sup>, Marina Colombi<sup>4</sup>, Francesco Brancati<sup>1,3</sup>✉ and Marco Ritelli<sup>4</sup>

© The Author(s), under exclusive licence to European Society of Human Genetics 2022

Pathogenic variants in *TGFBR1* are a common cause of Loey-Dietz syndrome (LDS) characterized by life-threatening aortic and arterial disease. Generally, these are missense changes in highly conserved amino acids in the serine-threonine kinase domain. Conversely, nonsense, frameshift, or specific missense changes in the ligand-binding extracellular domain cause multiple self-healing squamous epithelioma (MSSE) lacking the cardiovascular phenotype. Here, we report on two novel variants in the penultimate exon 8 of *TGFBR1* were identified in 3 patients from two unrelated LDS families: both were predicted to cause frameshift and premature stop codons (Gln448Profs\*15 and Cys446Asnfs\*4) resulting in truncated *TGFBR1* proteins lacking the last 43 and 56 amino acid residues, respectively. These were classified as variants of uncertain significance based on current criteria. Transcript expression analyses revealed both mutant alleles escaped nonsense-mediated mRNA decay. Functional characterization in patient's dermal fibroblasts showed paradoxically enhanced TGF $\beta$  signaling, as observed for pathogenic missense *TGFBR1* changes causative of LDS. In summary, we expanded the allelic repertoire of LDS-associated *TGFBR1* variants to include truncating variants escaping nonsense-mediated mRNA decay. Our data highlight the importance of functional studies in variants interpretation for correct clinical diagnosis.

*European Journal of Human Genetics* (2023) 31:596–601; <https://doi.org/10.1038/s41431-022-01279-4>

## INTRODUCTION

Loey-Dietz syndrome (LDS; OMIM PS609192) is an autosomal dominant condition mainly characterized by aortic aneurysm with arterial tortuosity, hypertelorism, bifid uvula [1]. Despite this classical triad, multiorgan involvement can be observed with craniofacial, skeletal, cutaneous, and immunological features. Major life-threatening complications include aortic aneurysm and dissection but also widespread and aggressive arterial aneurysms [2].

LDS is genetically heterogeneous with pathogenic variants in six genes, specifically *TGFBR1*, *TGFBR2*, *SMAD3*, *TGFB2*, *TGFB3* and *SMAD2*, causing overlapping subtypes nosologically classified as LDS1-6, respectively [3]. The presence of arterial aneurysm or dissection is not sufficient for the diagnosis of LDS and a clear pathogenic genetic variant is required, highlighting the importance of the molecular diagnosis and variant interpretation [4].

Among LDS-causative genes, *TGFBR1* variants account for about one third of cases with over 100 distinct variants reported in the HGMD database. Up to now, all *TGFBR1* pathogenic alleles

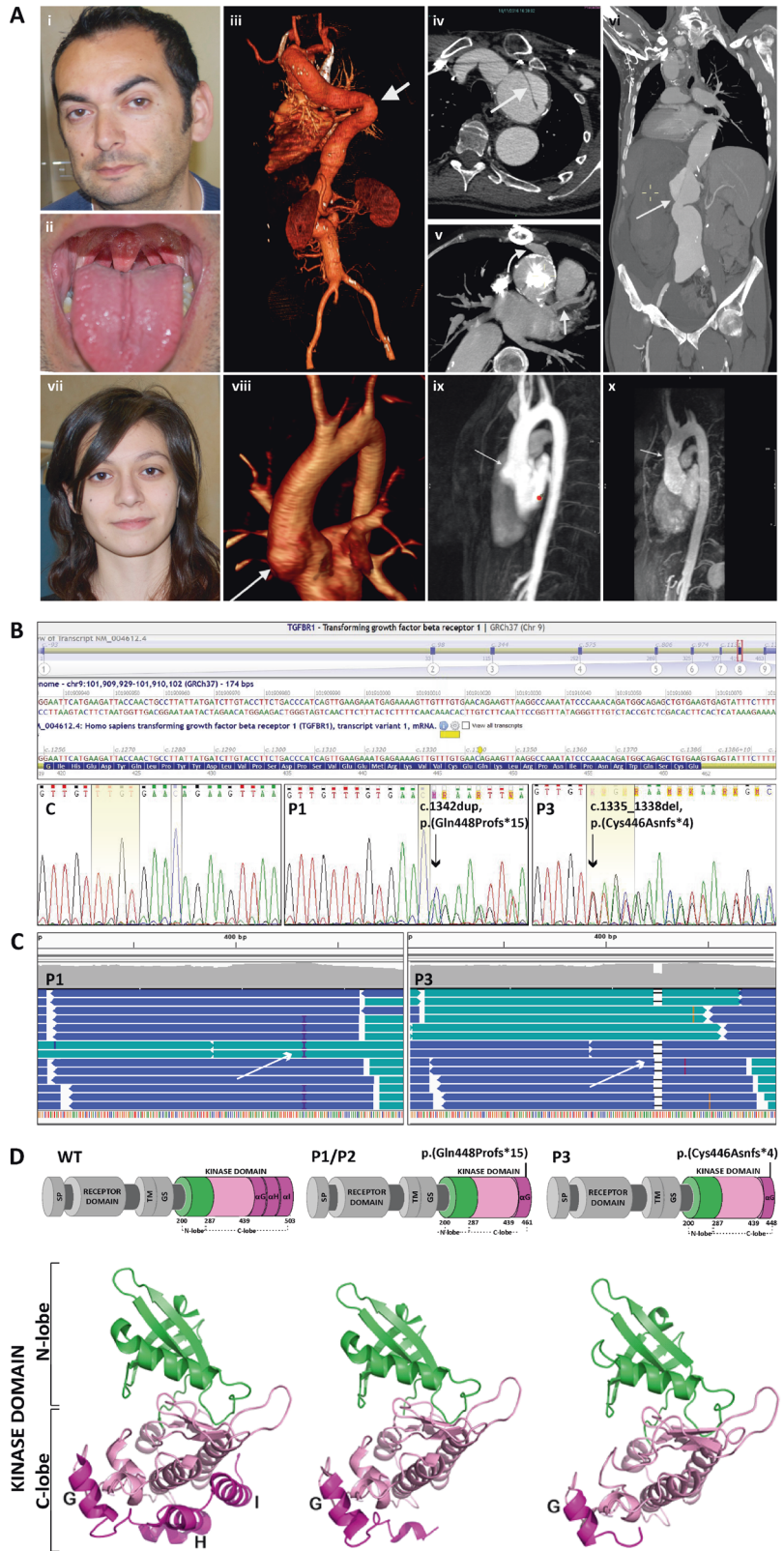
associated to LDS are missense substitutions located in, or immediately flanking, the evolutionarily conserved serine/threonine kinase (STK) domain and affect the kinase function as shown by *in vitro* overexpression studies [5]. It is worthy of note that loss of function mutations in TGF $\beta$  signaling components, including *TGFBR1*, ultimately lead to a paradoxical increase in downstream signaling *in vivo* [6–8]. Accordingly, TGF $\beta$  receptor knock-in LDS mouse models, but not haploinsufficient mice, recapitulated craniofacial, skeletal and vascular manifestations of LDS with clear evidence of TGF $\beta$  signaling upregulation in the aorta [9].

A specific subset of *TGFBR1* alleles causes a distinct disease, termed multiple self-healing squamous epithelioma (MSSE; OMIM#132800), featuring multiple skin tumors like squamous carcinomas, which invade locally and then regress spontaneously leaving harming scars [10]. In particular, MSSE results from *TGFBR1* nonsense or truncating changes, distributed throughout the gene or discrete missense alterations affecting the ligand-binding extracellular domain [11]. Notably, MSSE lacks the vascular phenotype seen in LDS, hence the importance of proper

<sup>1</sup>Human Functional Genetics Laboratory, IRCCS San Raffaele Roma, Rome, Italy. <sup>2</sup>Università Telematica San Raffaele, Rome, Italy. <sup>3</sup>Department of Life, Health, and Environmental Sciences, University of L'Aquila, L'Aquila, Italy. <sup>4</sup>Division of Biology and Genetics, Department of Molecular and Translational Medicine, University of Brescia, Brescia, Italy. <sup>5</sup>Clinical Genetics Unit, Department of Women and Children's Health, University of Padova, Padua, Italy. <sup>6</sup>IRP Città della Speranza, Padua, Italy. <sup>7</sup>Laboratory of Molecular and Cell Biology, Istituto Dermatologico dell'Immacolata IDI-IRCCS, Rome, Italy. <sup>8</sup>Department of Cardiac Surgery, European Hospital, Rome, Italy. <sup>9</sup>These authors contributed equally: Paola Fortugno, Rosanna Monetta. ✉email: francesco.brancati@univaq.it

Received: 21 October 2022 Accepted: 19 December 2022

Published online: 4 January 2023



interpretation of newly identified *TGFBR1* variants in clinical settings.

Here, we describe two independent families with typical LDS phenotypes carrying distinct frameshift variants in the

penultimate exon of *TGFBR1*. We showed that both genetic alterations escaped nonsense-mediated mRNA decay (NMD) and led to paradoxical upregulation of the TGFβ signaling pathway, substantiating a disease-causative role in LDS.

**Fig. 1 Clinical, molecular and protein modeling data of the herein reported families harboring two distinct truncating variants in the *TGFBR1* gene.** **A** Clinical and instrumental findings in family 1. Patient P1 (proband) (i–vi). (i) Facial appearance with hypertelorism at the age of 45 years, (ii) midline raphe of tongue and uvula. (iii–vi) Total body computed tomography angiographies documented tortuosity of the entire aorta and tight kinking at age 41 years (iii), dissection of the aortic arch (iv), left and right coronary dilatation (v, straight and curve arrows, respectively) at 44 years, extension of the dissection at age 47 years with involvement of supra-aortic branches and abdominal aorta (vi) and left renal occlusion (arrow). Patient P2 (vii–x). (vii) Facial gestalt with hypertelorism at the age of 20 years. (viii–x) Magnetic resonance angiographies performed at age 25 years showed aortic root dilatation before (viii and ix) and after surgery (x). **B** Molecular results. Sequence electropherograms showing the c.1342dup and c.1335\_1338del variants in *TGFBR1* identified in P1 and P3, respectively. Electropherogram relative to the non-affected P3's father is shown as normal control (C). Above, graphical representation of the exon 8 sequence of *TGFBR1* (NM\_004612.4, NP\_004603.1) obtained using Alamut Visual 2.15 software. The position of the two variants is shown with a yellow circle and box, respectively. **C** *TGFBR1* transcript analysis. Transcript analysis by deep sequencing of a *TGFBR1* amplicon encompassing exons 5–9 using cDNA from P1 and P3 peripheral lymphocytes. Alignment of the BAM files showing escape from NMD. On the left, patient P1 analysis: 110752 total reads, of which 68934 harboring the c.1342dup variant (62%). On the right, patient P3 analysis: 115,930 total reads, of which 49,522 harboring the c.1335\_1338del variant (43%). **D** Protein modeling of the *TGFBR1* variants. Above, schematic representation of the wild-type *TGFBR1* protein as compared to the two predicted truncated forms lacking the last 43 (Gln448Profs\*15) or 56 (Cys446Asnfs\*4) amino acid residues. Below, three-dimensional structure modeling of the cytoplasmic kinase domain of wild-type and mutant *TGFBR1* (residues 200–503; PDB code: 1VJY). N-terminal lobe (residues 200–286) and the C-terminal lobe (residues 287–503) are displayed in green and pink, respectively. The GHI helical subdomain (residues 439–503), belonging to the C-terminal lobe and almost completely missing in both mutants, is shown in magenta. WT wild-type, SP signal peptide, TM transmembrane domain, GS glycine- and serine-rich sequence domain.

## METHODS

Detailed methodologies relative to genetic investigations, ethical compliance, *TGFBR1* expression analyses and in silico and in vitro functional studies are available in the supplementary material.

## RESULTS

### Family 1

Patient P1 was born at term from healthy non-consanguineous parents and presented cleft palate and bilateral inguinal hernia. At age 10, he underwent the first surgical treatment for aortic root aneurysm followed in the next years by several other aortic surgeries. He died at the age of 48 due to a sudden rupture of an abdominal aorta aneurysm. Additional vascular findings included arterial tortuosity and ectasia of both carotid artery bifurcations. DXA scan documented decreased bone mineral density at age 42. Physical examination at age 45 showed ocular hypertelorism, midline raphe of tongue and uvula, low muscle bulk, pectus excavatum, severe scoliosis, limited hip external rotation, pes planus, and laxity of small joints. Cutaneous findings included facial milia, thin skin with visible subcutaneous veins and skin striae (Fig. 1A).

His daughter (P2) reported, from age 14, progressive aortic root dilatation, surgically replaced at age 25 due to a 40 mm aneurysm. Involvement of other vascular defects was excluded. Physical examination at age 20 showed ocular hypertelorism, broad uvula with a median raphe, velvety and slightly translucent skin with visible subcutaneous veins, high grade myopia and decreased bone mineral density. Musculoskeletal findings consisted of combined thumb and wrist signs (Fig. 1A).

NGS of P1 using a custom panel including all LDS-associated genes led to the identification of a heterozygous c.1342dup variant in *TGFBR1*, also present in P2 but not in his older unaffected son. The variant, confirmed at Sanger sequencing, was predicted to cause a translational frameshift and a premature stop codon p.(Gln448Profs\*15) (Fig. 1B). WES analysis was also performed and only one additional candidate variant was identified in the *RYR1* gene after filtering strategy (Table S1 and S2). None of the *RYR1* associated phenotypes was diagnosed in P1.

### Family 2

The proband (P3) was born after a pregnancy obtained by assisted reproduction techniques and egg-donation (no donor data was available). Physical examination at age 5 showed mild hypertelorism with downslanted palpebral fissures, a long face with malar hypoplasia, pointed chin, high-arched palate (with normal uvula), and dental crowding. She had pectus excavatum and displayed

strikingly long fingers of hands and feet. An echocardiography at age 3 showed normal anatomy, with a mild dilation of the aortic root (Z-score +2.27).

Custom NGS analysis, performed using a panel alike that employed for family 1, revealed a heterozygous c.1335\_1338del variant in *TGFBR1*, confirmed by Sanger sequencing (Fig. 1B). The variant was located in exon 8 and led to frameshift and premature termination [p.(Cys446Asnfs\*4)], was absent in her father, while maternal DNA was not available for segregation analysis. Clinical exome sequencing was performed to exclude additional variants in relevant genes (Tables S1 and S2).

### Bioinformatics analysis

Analysis of the novel c.1342dup and c.1335\_1338del variants by the Alamut visual software revealed no entries in all databases analyzed. However, c.1342dup variant was mentioned in the ClinVar database (RCV001209677.2), classified of uncertain significance (VUS) and associated to a “familial case of thoracic aortic aneurysm and dissections” without further information.

Both variants are predicted to result in truncated *TGFBR1* proteins within the STK domain, lacking the highly conserved GHI helical sub-domain, involved in regulation of kinase activity, oligomerization, and interaction with substrates (Fig. 1D).

Gene variant databases were interrogated for similar *TGFBR1* alterations in the ultimate or penultimate exons and other 4 variants leading to a frameshift and prematurely truncated protein were identified (Table S3). Almost all of them were associated to an unspecified “cardiovascular phenotype” and classified as VUS or likely pathogenic.

### Functional analysis

The relative abundance of wild-type and mutant transcripts was assessed through deep sequencing of a 593 bp *TGFBR1* amplicon encompassing both variants. In cDNA obtained from P1 and P3 leukocytes, the c.1342dup and the c.1335\_1338del variants were called by 62 and 43% of the total reads, respectively, thus demonstrating that both mutant alleles escaped NMD (Fig. 1C).

WB analysis failed to reveal the truncated form in P1 fibroblasts. However, total *TGFBR1* protein levels were not significantly reduced (Fig. 2A).

Both canonical and non-canonical TGF $\beta$  signaling pathways were explored in P1 dermal fibroblasts. A constitutive elevation of the levels of phosphorylated SMAD2 and p38-MAPK was observed by IF, and an approximately 7.5-fold ( $p < 0.001$ ) and 1.6-fold ( $p < 0.05$ ) increase of the p-p38/p38 and p-ERK/ERK ratios, respectively, was assessed by WB (Fig. 2B, C).

Finally, in line with increased myogenic differentiation in LDS fibroblasts, about 30% more P1 fibroblasts than controls showed a

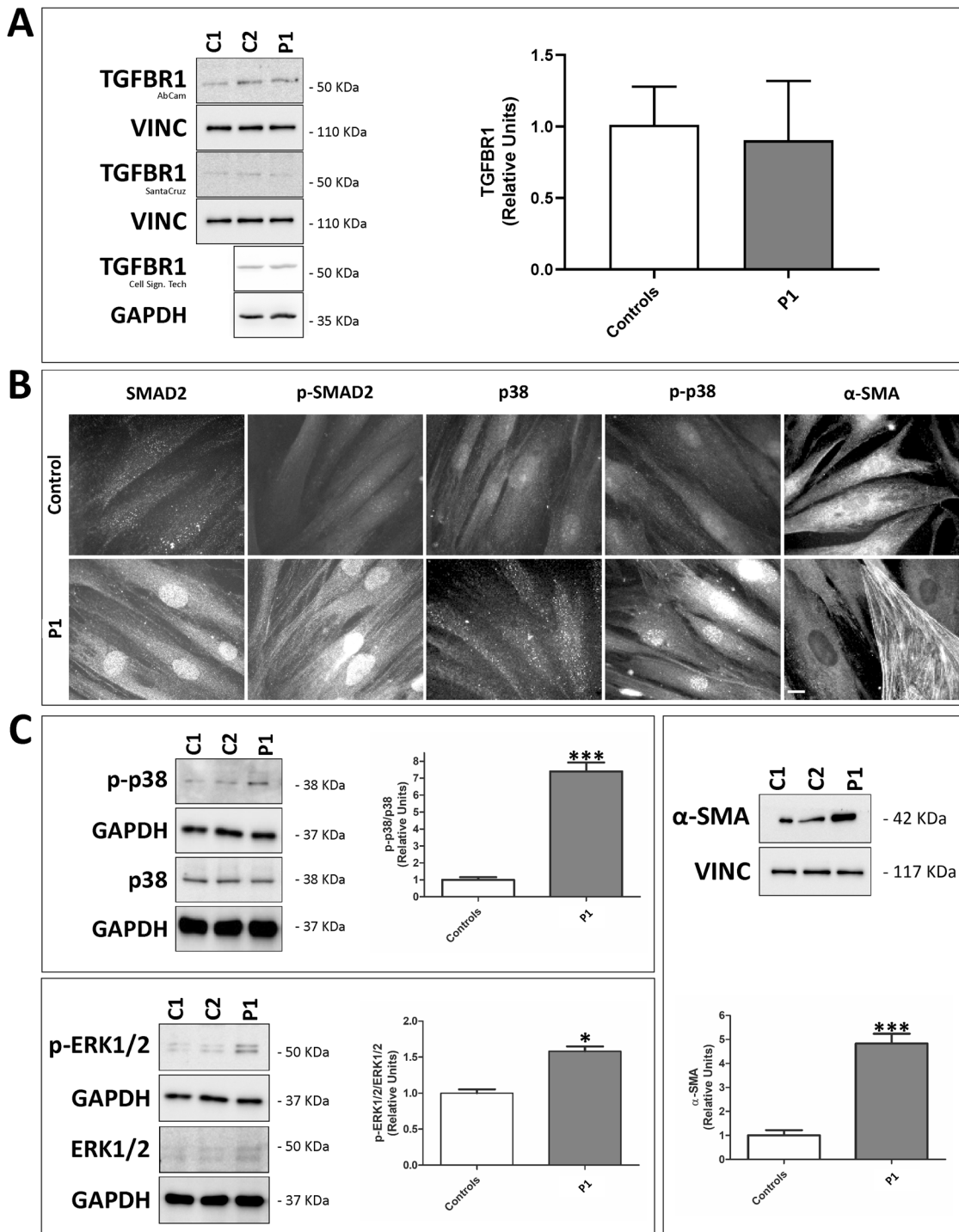


**Fig. 2 Molecular and cellular studies.** **A** Representative images of WB results for TGFBR1 performed on fibroblasts from P1 and two healthy donors (C1, C2) with three different antibodies directed to distinct TGFBR1 regions: a mouse monoclonal antibody directed to aa 26–125 (SantaCruz); two rabbit polyclonal antibodies directed to aa 150–250 and the central intracellular region (AbCam and Cell Signaling Technology, respectively). Vinculin (VINC) and GAPDH were used as internal loading control for normalization. The graph shows quantitative results (presented as fold change) of the TGFBR1 levels achieved from 6 independent experiments, which revealed no significant differences between patient and control cells. Error bars represent the mean value  $\pm$  SD. **B** IF of SMAD2 and its phosphorylated form (p-SMAD2; pS465/S467), p38 and its phosphorylated form (p-p38, pT180/Y182), and  $\alpha$ -SMA demonstrating enhanced canonical and non-canonical TGF $\beta$  signaling and increased cytoskeleton-associated  $\alpha$ -SMA in P1 dermal fibroblasts as compared to a representative control. The experiments were repeated three times and images of control cells are representative of two different cell strains; scale bar: 8  $\mu$ m. **C** Representative images of WB results for ERK1/2 and p-ERK1/2 (pT202/Y204), p38 and p-p38 (pT180/Y182), and  $\alpha$ -SMA performed on fibroblasts from P1 and two healthy donors (C1, C2). GAPDH and vinculin (VINC) were used as internal loading control for normalization. The graphs show quantitative results (presented as fold change) of the p-ERK1/2/ERK1/2 ratio, p-p38/p38 ratio, and  $\alpha$ -SMA levels achieved from 3 independent experiments, which confirmed increased TGF $\beta$  signaling and  $\alpha$ -SMA levels in patient's cells. Error bars represent the mean value  $\pm$  SD (\* $p$  < 0.05; \*\*\* $p$  < 0.001).

well organized  $\alpha$ -SMA cytoskeleton. WB analysis confirmed an about 5-fold increase ( $p < 0.001$ ) of  $\alpha$ -SMA levels in patient fibroblasts (Fig. 2B, C).

## DISCUSSION

We describe 3 patients from two families with typical features of LDS bearing two frameshift variants in *TGFBR1*, c.1342dup (Gln448Profs\*15) and c.1335\_1338del (Cys446Asnfs\*4), both located in the penultimate exon of the gene. Although this type of changes is archetypal of MSSE rather than LDS, we found similar truncating variants in online databases identified in patients with cardiovascular phenotype: 4 in the penultimate exon and 1 in the last (Table S3), including the c.1342dup variant in ClinVar (RCV001209677.2) associated to a “familial case of thoracic aortic aneurysm and dissections” with no further descriptions. Notably, all these changes were classified as VUS or at most likely pathogenic according to current guidelines [12]. Truncating variants, expected to result in loss of function by premature protein truncation or NMD, have not been clearly established as a mechanism of disease for LDS. Indeed, genetic alterations in the *TGFBR1* gene result in LDS or MSSE by different mechanisms: missense variants located in (or close to) the STK domain and affecting the kinase activity are associated to LDS, while haploinsufficiency resulting from nonsense or frameshift variants, as well as missense variants in the ligand-binding extracellular domain, are associated to MSSE [10, 11, 13]. Both frameshift variants herein identified escaped NMD likely due to their position at the 3' end of the gene. 3D modeling predicted truncated proteins with impaired kinase activity, although we could not detect the truncated form by WB analysis. Interestingly, the total amount of TGFBR1 was not found to be reduced as it would be expected. In addition, we observed activation of the canonical and non-canonical TGF $\beta$  signaling pathways, as shown by a constitutive increase of the levels of phosphorylated SMAD2, p38-MAPK and ERK1/2. Also, we detected an increase of  $\alpha$ -SMA levels in patient's cells, indicative of increased myogenic differentiation in LDS fibroblasts [7]. These results are in line with the paradoxical activation of the TGF $\beta$  pathway reported in LDS caused by loss of function mutations [14].

In summary, we expanded the allelic repertoire of *TGFBR1* associated to LDS to include truncating variants in the last exons escaping NMD. Our findings highlight the importance of integrated clinical genetic databases with functional data for correct interpretation of genomic variants and we propose NMD analysis to evaluate pathogenicity of truncating variants of uncertain significance.

## DATA AVAILABILITY

The novel *TGFBR1* variants identified in this study were submitted to the Leiden Open Variation Database (LOVD; <https://databases.lovd.nl/shared/genes/TGFBR1>), with IDs: #0000785357 and #0000785358. Additional data and materials are available from the corresponding author on reasonable request, subject to compliance with our obligations under human research ethics.

## REFERENCES

- Loeys BL, Dietz HC Loeys-Dietz Syndrome. 2008 Feb 28 [Updated 2018 Mar 1]. In: Adam MP, Ardinger HH, Pagon RA, et al., editors. GeneReviews® [Internet]. Seattle (WA): University of Washington, Seattle; 1993-2022.
- Van Laer L, Dietz H, Loeys B. Loeys-dietz syndrome. *Adv Exp Med Biol*. 2014;802:95–105.
- Camerota L, Ritelli M, Wischmeijer A, Majore S, Cinquina V, Fortugno P, et al. Genotypic categorization of Loeys-Dietz syndrome based on 24 novel families and literature data. *Genes (Basel)*. 2019;10:764.
- MacCarrick G, Black JH 3rd, Bowdin S, El-Hamamsy I, Frischmeyer-Guerrero PA, Guerrero AL, et al. Loeys-Dietz syndrome: A primer for diagnosis and management. *Genet Med*. 2014;16:576–87.

- Cardoso S, Robertson SP, Daniel PB. TGFBR1 mutations associated with Loeys-Dietz syndrome are inactivating. *J Recept Signal Transduct*. 2012;32:150–5.
- Loeys BL, Chen J, Neptune ER, Judge DP, Podowski M, Holm T, et al. A syndrome of altered cardiovascular, craniofacial, neurocognitive and skeletal development caused by mutations in TGFBR1 or TGFBR2. *Nat Genet*. 2005;37:275–81.
- Cozijnsen L, Plomp AS, Post JG, Pals G, Bogunovic N, Yeung KK, et al. Pathogenic effect of a TGFBR1 mutation in a family with Loeys–Dietz syndrome. *Mol Genet Genom Med*. 2019;7:e00943.
- Hara H, Takeda N, Fujiwara T, Yagi H, Maemura S, Kanaya T, et al. Activation of TGF- $\beta$  signaling in an aortic aneurysm in a patient with Loeys-Dietz syndrome caused by a novel loss-of-function variant of TGFBR1. *Hum Genome Var*. 2019;6:eCollection 2019.
- Gallo EM, Loch DC, Habashi JP, Calderon JF, Chen Y, Bedja D, et al. Angiotensin II-dependent TGF- $\beta$  signaling contributes to Loeys-Dietz syndrome vascular pathogenesis. *J Clin Invest*. 2014;124:448–60.
- Goudie DR, D'Alessandro M, Merriman B, Lee H, Szevevényi I, Avery S, et al. Multiple self-healing squamous epithelioma is caused by a disease-specific spectrum of mutations in TGFBR1. *Nat Genet*. 2011;43:365–71.
- Fujiwara T, Takeda N, Hara H, Morita H, Kishihara J, Inuzuka R, et al. Distinct variants affecting differential splicing of TGFBR1 exon 5 cause either Loeys–Dietz syndrome or multiple self-healing squamous epithelioma. *Eur J Hum Genet*. 2018;26:1151–8.
- Richards S, Aziz N, Bale S, Bick D, Das S, Gastier-Foster J, et al. Standards and guidelines for the interpretation of sequence variants: A joint consensus recommendation of the American College of Medical Genetics and Genomics and the Association for Molecular Pathology. *Genet Med*. 2015;17:405–24.
- Fujiwara T, Takeda N, Ishii S, Morita H, Komuro I. Unique mechanism by which TGFBR1 variants cause 2 distinct system diseases- loeys-dietz syndrome and multiple self-healing squamous epithelioma. *Circ Rep*. 2019;1:487–92.
- Akhurst RJ. The paradoxical TGF- $\beta$  vasculopathies. *Nat Genet*. 2012;44:838–9.

## ACKNOWLEDGEMENTS

We wish to thank the families for kind availability to participate to this study and for allowing us to share these findings within the scientific community. This work is dedicated to the memory of Letizia Camerota, brilliant and devoted medical geneticist of L'Aquila University, Italy.

## AUTHOR CONTRIBUTIONS

PF, RM, VC, NZ, LDL, EDD and RI performed mRNA expression analyses, functional studies, immunofluorescence microscopy and western blotting; VC, CR, FBo, ADD, LS and MR performed the molecular genetic investigations; CR, FBo and CDL performed the bioinformatic analysis of the data and revised the literature; CDL, RDP, LS and FBr, performed the clinical assessment; FA performed protein modeling studies; EDC performed the imaging assessment; MC, FBr and MR had a major role in acquiring and processing clinical and molecular data, in the study concept and in the revision and finalization of the manuscript with all the authors' input. All authors read and approved the final manuscript.

## FUNDING

VC, NZ, MC, and MR, also thank the Fazzo Cusan family for its generous support. LS is supported by a grant from Fondazione IRP Città della Speranza, Padova. FBr and FA are funded by intramural Grant of the University of L'Aquila (FFO2020). FBr and PF were supported by funding of the Italian Ministry of Health [ricerca corrente].

## COMPETING INTERESTS

The authors declare no competing interests.

## ETHICS STATEMENT

The Internal Review Board of the University of L'Aquila approved this study (Project code PGR00919). Written informed consent for genetic testing and use of peripheral blood, skin biopsy, and clinical data for research and publication purposes were obtained from all the patients or their legal guardians.

## ADDITIONAL INFORMATION

**Supplementary information** The online version contains supplementary material available at <https://doi.org/10.1038/s41431-022-01279-4>.

**Correspondence** and requests for materials should be addressed to Francesco Brancati.

**Reprints and permission information** is available at <http://www.nature.com/reprints>

**Publisher's note** Springer Nature remains neutral with regard to jurisdictional claims in published maps and institutional affiliations.

Springer Nature or its licensor (e.g. a society or other partner) holds exclusive rights to this article under a publishing agreement with the author(s) or other rightsholder(s); author self-archiving of the accepted manuscript version of this article is solely governed by the terms of such publishing agreement and applicable law.